*Available online at*www.scholarsresearchlibrary.com

Scholars Research Library

Archives of Applied Science Research, 2015, 7 (2):39-49
(http://scholarsresearchlibrary.com/archive.html)

ISSN 0975-508X
CODEN (USA) AASRC9

Spectral, optical, thermal and mechanical studies of metal halide co-ordinate pyridinium derivatives

A. Philominal[1], M. Thenmozhi[2,3], M. N. Ponnuswamy[3] and S. Dhanuskodi[1*]

[1]School of Physics, Bharathidasan University, Tiruchirappalli, India
[2]Centre for Nanotechnology and Advanced Biomaterials (CeNTAB), School of Chemical and Biotechnology, SASTRA University, Thanjavur, India
[3]Centre of Advanced Study in Crystallography and Biophysics, University of Madras, Guindy Campus, Chennai, India

---

ABSTRACT

Metal – organic coordination compounds dichloridobis(1-ethyl-2, 6-dimethylpyridinium-4-olate-κO) zinc (II) (EDMPZC) and dibromidobis(1-ethyl-2, 6-dimethylpyridinium-4-olate-κO) zinc (II) (EDMPZB) was designed and synthesized and single crystals was grown by solvent evaporation technique. Both the complexes were characterized by single crystal X-ray diffractometry, FTIR, FT NMR and elemental analyses. Optical transmittance window and the lower cutoff wavelength (262 nm for EDMPZC and 263 nm for EDMPZB) were identified from the linear optical studies. Laser induced surface damage threshold of EDMPZC and EDMPZB are 29.25 GW/cm^2 and 71.16 GW/cm^2 respectively. Thermal stability of the complexes was performed by Thermogravimetric / Differential Thermal Analysis (TG/DTA), and Differential Scanning Calorimetry (DSC) techniques.

Keywords: Optical Materials; Crystal Growth; Fourier transform Infrared Spectroscopy; Differetial Thermal Analysis (DTA); Differential Scanning Calorimetry (DSC); Crystal Structure

---

INTRODUCTION

Extensive research in the field of nonlinear optics has revealed that semiorganic compounds possess a high degree of nonlinearity, tailor made synthetic flexibility and scope to alter their properties by functional substituitions make their materials highly attractive. It also finds wide range of applications in optical device fabrication suitable for information processing, optical switching, optical frequency conversion and telecommunications [1-3]. Recent success in the constructive of potentially useful metal complexes of highly polarizable organic molecule can be called as metal-organics. It using strong and highly directional metal-ligand co-ordination bonds, possesses appreciable physical properties such as high damage resistance. The common wisdom has been that optical materials should have a large charge transfer and the optical transparency with less dislocation density. The rationalized approach for the design and synthesis of metal-organic frameworks (MOFs) with desirable and predictable properties remains underdeveloped [4-10]. As reported previously by Fur et al [11] and Dhanuskodi et al [12] 1-ethyl-2, 6-dimethyl-4(1H) pyridinone trihydrate (EDMP.3H_2O) is an efficient and versatile organic building unit for the construction of co-ordination architectures and a variety of MOFs with interesting structure, topologies and properties have been obtained [13-15]. The addition of metal halides (MX_2; M = Zn, X = Cl and Br) with EDMP.3H_2O leads to the centrosymmetric arrangement of these molecules in the crystal and thus χ_2 vanishes while

χ_3 possible with the crystals. The crystal structure of EDMPZC and EDMPZB was reported by Thenmozhi et al [16-17]. Philominal et al [18] reported the optical limiting characteristics of EDMPZC. In this paper, we report the design and synthesis of metal organic frameworks (MOFs), EDMPZC and EDMPZB and are characterized by elemental analysis, infrared and NMR spectroscopy, UV-Vis spectroscopy, X-Ray diffractometry, thermogravimetry and laser induced surface damage studies.

MATERIALS AND METHODS

The complexes were prepared by the reaction of ZnX_2 (X - Cl, Br) with 1-ethyl-2, 6-dimethyl -4(1H) pyridinone trihydrate (EDMP.$3H_2O$) in the molar ratio 1:2 respectively in aqueous medium. The starting material EDMP.$3H_2O$ had been prepared by following the synthetic method reported by Garratt [19]. The salts were further purified by the repeated recrystallization process in triple distilled water. The solubility test was carried out by mass gravimetric method in the temperature range 30° - 55°C and water is the suitable solvent for the growth of good quality crystals. Single crystals of EDMPZC and EDMPZB were harvested after a typical growth period of 15 days from the saturated aqueous solution at 30 °C by the slow evaporation of the solvent.

The percentage composition of the elements carbon, hydrogen and nitrogen present in the synthesized compounds were determined by CHN elemental analysis in an Elementar systeme Model Vario EL III instrument.

To analyze three dimensional arrangement of the molecules in the crystal, the single crystal X-ray diffraction analysis of EDMPZC and EDMPZB were recorded using a Bruker SMART APEXII area-detector diffractometer with MoKα (λ =0.70713 Å) radiation at 293 K. The data were integrated using APEX2 and SAINT for both the structures EDMPZC and EDMPZB. Correction for absorption and decay was applied using SADABS [G. M. Sheldrick, SADABS, University of Gottingen, Germany]. All calculations were performed using SHELXL 97 [G. M. Sheldrick, 2008]. The structure was solved by direct methods and full-matrix least-squares refinements were performed on F^2 using all unique reflections. Presence of all nonhydrogen atoms and hydrogen atoms were refined with anisotropic and isotropic atomic displacement factors. Graphical representation of the molecular structure and the packing diagram were obtained using ORTEP-3 [Farrugia, 1997]. FTIR spectra were recorded using a JASCO 460 PLUS FTIR spectrometer in the range 400 - 4000 cm^{-1} by KBr pellet technique at 300 K. The proton and carbon configurations of the synthesized compounds were identified by ^1H (300 MHz, D_2O, 300 K) and ^{13}C (300 MHz, $CDCl_3$, 300 K) NMR spectra and recorded using a JEOL Model GSX 400, Bruker FT NMR spectrometer. The optical absorption spectrum was recorded using a Varian Cary 5E UV-Vis Spectrometer in the range 200 – 800 nm in MeOH solution.

Thermo gravimetric/differential thermal analyses (TG/DTA) were carried out using a Seiko Make instrument in the temperature range 28 ° to 820 °C at a heating rate of 20.00 °C/min in nitrogen atmosphere. DSC measurements were carried out using a Mettler Toledo DSC 822^e differential scanning calorimeter in the temperature range 50° - 400 °C. The laser damage threshold of a grown crystal of EDMPZC and EDMPZB about 5 mm of diameter and 2 mm thickness was measured using a Q-switched Nd: YAG laser (1064 nm, 10 ns, 10 Hz). The laser beam was focused using a focusing lens (20 cm) and the measured focal spot size was 259 µm. A photo diode was used to identify the pulse-to-pulse variation of the incident and sufficient time was allowed to stabilize the output power of the laser. The scattered second harmonic signal from the crystal was collected using a lens and monitored using a monochromator, PMT and CRO.

RESULTS AND DISCUSSION

3.1 Elemental Analysis

The percentage composition of elements C, H and N present in the EDMPZC and EDMPZB complexes with EDMP.$3H_2O$ are presented in **Table 1a** and the observed and computed (in parenthesis) values are in good agreement.

3.2 Single Crystal X-ray Diffraction

Diffraction topography has provided information on the perfection of the crystal used in industry as integral part of the devices. The crystal structures were solved by direct method and computerized by the full matrix least square technique using the SHELXL program. The crystallographic data and structure refinement parameters of EDMPZC and EDMPZB are given in **Table 1b**.

The ORTEP plot of the molecules EDMPZC and EDMPZB are shown in **Figs. 1a & 1b**. Both the crystal structures are isostructural in nature. The pyridinium rings are planar and oriented each other at angles of 67.79 (8) ° for (EDMPZC) and 34.4 (2) ° for (EDMPZB). The Zn atom which lies on a twofold axis shows a distorted tetrahedral geometry in both the chloro (EDMPZC) and bromo (EDMPZB) derivatives. The pyridinium rings assume a substantial degree of quinoidal character, which is reflected in the variation of bond lengths (**Table 2a and 3a**) [20].

The methyl substituents at C2, C6, C12 and C16 are nearly coplanar with the corresponding pyridinium rings, which are evident from the torsion angles [C9—C2—N1—C6 = 176.99 (16)°; C10—C6—N1—C2 = -175.51 (17)°; C19—C12—N11—C16 = 178.46 (18)°; C20—C16—N11—C12 = -178.4 (2)°] for molecule (EDMPZC) and [C9—C2—N1—C6 = 178.0 (4)°; C10—C6—N1—C2 = -178.4 (4)°; C19—C12—N11—C16 = 179.9 (4)°; C20—C16—N11—C12 = -178.2 (4)°] for molecule (EDMPZB), respectively. Both the ethyl groups attached at N1 and N11 are approximately perpendicular to pyridinium ring, which can be seen from the torsion angles [C8—C7—N1—C2 = 93.7 (2)°; C18—C17—N11—C12 = 90.0 (2)°] for (EDMPZC) and [C8—C7—N1—C2 = -88.5 (6)°; C18—C17—N11—C12 = 87.6 (5)°] for (EDMPZB). The sum of the bond angles around the protonated nitrogen atoms N1 [360.0° (EDMPZC); 359.8° (EDMPZB)] and N11 [359.99° (EDMPZC); 360.0° (EDMPZB)] of both the pyridinium rings is in accordance with sp^2 character [21].

3.2.1 EDMPZC

The packing of the molecules in crystal structure is promoted by the existence of weak C—H···O, C—H···Cl and π-π types of intermolecular interactions in addition to van der Waals forces. The C8—H8A···O1 interaction leads to the formation of $R_2^2(16)$ centrosymmetric dimer, viewed down *c*-axis is shown in **Fig. 2a**. The chlorine atom Cl1 which acts as an acceptor in a linear fashion for the methyl group hydrogens from the neighbouring molecule [**Table 2b**]. The C13—H13···Cl2 intermolecular interaction also contributes to the crystal packing, which forms zig–zag chain directed along *c*-axis, as shown in **Fig. 2b**. The crystal structure is further augmented by π-π interaction between adjacent pyridinium rings [Cg1(x, y, z) ···Cg1 (-x, y, 1/2-z) = 3.669 (1) Å; where Cg1 is the centroid of the (N1—C6) ring, **Fig.2a**].

3.2.2 EDMPZB

The packing of the molecules is reinforced by both π-π intermolecular and C—H···O intramolecular interactions. A couple of π–π interactions [Cg1(x, y, z)···Cg1(2-x, 1-y, -z) = 3625 (3) Å; where Cg1 is the centroid of the (N1—C6) ring] and [Cg2(x, y, z)···Cg2(1-x, 1-y, 1-z) =3.711 (2) Å; where Cg2 is the centroid of the (N11—C16) ring] between the pyridinium rings are observed. Both the π–π interactions run diagonally along the *ac* plane, as an infinite continuous chain, as shown in **Fig. 3**. A weak C5—H5···O2 intramolecular interaction is also observed [**Table 3b**].

3.3 FTIR Spectroscopy

FTIR spectra are used to elucidate the molecular structure and to identify the various functional groups presence in the synthesized compounds. The comparison of characteristic vibrational frequencies of EDMPZC, EDMPZB with EDMP are presented in **table 4**. Due to the introduction of metal ($ZnCl_2$ and $ZnBr_2$) into the EDMP entity, an overall shift can be observed in their characteristic vibrational frequencies. In EDMPZC and EDMPZB the H - bonded, O − H stretching frequency shows a broad band at 3429 cm^{-1} and 3443 cm^{-1} respectively, which leads to the formation of clathrate structure. The fundamental vibrational mode at frequencies 2976 cm^{-1} and 2992 cm^{-1} are due to the C − H stretching vibrations of methyl and ethyl group. The first overtone is identified at 1558 cm^{-1} and 1557 cm^{-1} for EDMPZC and EDMPZB respectively, whereas EDMP shows these at 3000 cm^{-1} and 1549 cm^{-1}. The C−H bending deformations (in-plane and out of plane) are observed at frequencies 1479 cm^{-1} and 729 cm^{-1} respectively. The C–H of CH_3 bending is observed at frequencies 1373 cm^{-1} and 1336 cm^{-1} respectively. It is also noted that the presence of Zn−O stretching at 452 cm^{-1} and 460 cm^{-1} for EDMPZC and EDMPZB confirms the formation of new compound whereas it is absent in EDMP.

3.4 FT NMR spectral Analysis

The proton - carbon configurations of EDMPZC and EDMPZB were elucidated by ^1H and ^{13}C NMR spectra. The comparison of shifts observed from ^1H and ^{13}C NMR spectra of EDMPZC and EDMPZB with the parent material EDMP.$3H_2O$ is illustrated in **Table 5.** From the ^1H NMR spectrum, the presence of water molecule has been noticed at δ = 4.690 ppm and δ = 4.683 ppm for EDMPZC and EDMPZB at the molecular level. The quartet (δ = 3.938 ppm) and triplet (δ = 1.140 ppm) reveal the presence of ethyl group. The singlets at δ = 2.290 ppm is due to methyl group whereas the shift at δ = 6.209 ppm is due to the aromatic hydrogen. From the ^{13}C NMR spectrum, The

presence of methyl group addresses the peaks at δ = 13.44 ppm and δ = 19.43 ppm. The signal at δ = 116.92 ppm is due to ethyl substitution. It is identified that the remarkable downfield shift in the carbonyl group by the presence of metal halide salts whereas the upfield shift for the substitution of halide salts and thus identifies the protonation site as nitrogen. Here, the Zn^{II} ion is coordinated by two Cl^- and Br^- ions for EDMPZC and EDMPZB and two O atoms of two Zwitterionic organic ligands in a distorted tetrahedral arrangement. The ethyl group attached to N1 and N11 are approximately perpendicular to pyridinium ring and the sum of the bond angles around the protonated nitrogen atoms N1 and N11 of both pyridinium rings are in accordance with sp^2 character. The carbon atoms of methyl substituents at C2, C6, C12 and C16, lie in the plane of the corresponding pyridinium rings, which are evident from the torsion angles. The packing of molecules in the unit cell is promoted by the existence of weak C—H··· O, C—H··· Cl and π-π types of intermolecular interactions. Further it confirms the absence of intermolecular hydrogen bonding in solution which usually shifts the peak towards the down field (δ = 12.00 to 10.00 ppm).

3.5 Optical Studies

High optical transmittance and lower cutoff wavelengths are very important properties for nonlinear optical crystals. The UV-Visible spectra of EDMPZC and EDMPZB show no remarkable absorption change in the spectral width. But the large transmittance window in the UV and visible region makes the candidates suitable for optoelectronic applications and the generation of higher harmonics using Nd: YAG laser through NLO phenomena. The comparison of optical parameters, lower cutoff wavelength and the optical transmittance window of some of the synthesized compounds are presented in **table 6**. It is evident that the addition of metal halides improves the transmittance window but instead there is no remarkable difference in the optical window among the complexes.

3.6 Thermal Analyses

The initial mass taken for the TG/DTA analysis of EDMPZC and EDMPZB complexes were 5.294 mg and 7.571 mg. From the thermogram of EDMPZC and EDMPZB, shown in **fig. 4a**, A sharp endothermic peak at 259°C and 253 ± 1 °C for EDMPZC and EDMPZB respectively confirms the melting point of the material at this temperature, whereas EDMP melts at 165 ± 1°C. The sharpness of the peak reveals the good crystallinity of the sample. At 434 °C EDMPZC loses its complete weight due to the breaking up of the molecule. In DTA of EDMPZB, an endothermic peak at 294.27 ˚C is due to the presence of metal in EDMPZB. This endotherm followed by a sharp exotherm at 385 °C in the DSC curve coincides with the major weight loss observed in the TGA curve. An endothermic peak at 503.4 °C shows the complete weight loss due to the breaking up of the molecules and the remaining of 5% weight only at 806 °C. From the DSC curve **(Fig. 4b)**, the presence of weight loss is observed in the region 45 - 108 °C, and the sharp endothermic peak shows the melting point of the material as 259 ± 1 °C and 253 ± 1 °C for both the complexes. Thus the results observed from the DSC and DTA clearly indicate the temperature stability of the materials.

3.7 Laser Induced Surface Damage Studies

Laser damage threshold is defined as the maximum permissible optical power to cause a breakdown of the material. According to Nakatani et al [23] the multiple shot (n-on-1) damage threshold is the minimum power level below which the crystal does not suffer damage after multiple shot pulses. The origin of laser induced damage is highly material dependent. The mean surface laser damage threshold of the grown crystals EDMPZC and EDMPZB were calculated by plotting the SHG output (mV) against input energy (mJ) of the beam (**Fig. 5**). It is observed that, the SHG output increases with increase of input energy and reaches a maximum at which damage occurs finally decreases with further increase of incident energy. The corresponding maximum energy was taken to calculate the power density (P) using the expression

$$P = \frac{E}{\tau \pi \omega_0^{\,2}} \qquad \text{---------- (1)}$$

Where E is the energy (mJ), τ is the pulse width and ω_0 is the radius of the spot. The laser damage threshold of EDMPZC and EDMPZB are estimated as 29.25 GW/cm^2 and 71.16 GW/cm^2 and it was compared with other complexes of EDMP (**table 6**). It is identified that, the addition of inorganics (metal halides MX_2; M = Zn, X = Cl and Br) in EDMP.$3H_2O$ (7.6 GW/cm^2) improves the damage resistance. Also it is noted that the addition of metal halides increases the laser damage than EDMP halides.

Fig. 5 Variation of SHG output against input energy for EDMPZC and EDMPZB

Table 1a: Elemental analysis

Compound	%C	%H	%N
	Observed (Computed)	Observed (Computed)	Observed (Computed)
EDMP.3H_2O [12]	52.23 (52.67)	10.61 (9.33)	6.59 (6.82)
EDMPZC	38.39 (35.38)	4.96 (4.95)	5.03 (4.60)
EDMPZB	23.31 (24.10)	3.59 (4.70)	3.03 (3.12)

Table 1b: Crystallographic data and structure refinement of EDMPZC and EDMPZB

Parameters	EDMPZC	EDMPZB
Empirical Formula	$C_{18}H_{26}Cl_2N_2O_2Zn$	$C_{18}H_{26}Br_2N_2O_2Zn$
M_r	438.68	527.60
Temperature (K)	293	293
Wavelength (Å)	0.71073	0.71073
Crystal system	Monoclinic	Triclinic
Space group	C2/c	Pī
Unitcell dimensions	a = 30.365 (2) Å b = 8.5366 (6) Å c = 15.7982 (12) Å β = 94.281 (4) °	*a* = 8.462 (1) Å *b* = 8.518 (1) Å *c* = 14.418 (3) Å α = 93.131 (6) °, β = 97.871 (7) °, γ = 90.210 (8) °
Volume	4083.7 (5) $Å^3$	1027.9 (2) $Å^3$
Z	8	2
Density (g/cm^3)	1.427	1.705
Absorption coefficient	1.48 mm^{-1}	5.10 mm^{-1}
Reflections collected	19140	16553
Independent reflections	5069 [R(int)=0.042]	16553 [R(int)=0.000]
Refinement method	Full-matrix least-squares on F^2	
Data/restraints/parameters	4248/0/233	13614/0/233
Goodness-of-fit on F^2	0.99	1.06
R indices [I>2σ(I)]	$R[F^2>2\sigma(F^2)]$=0.031 $wR(F^2)$=0.084	$R[F^2>2\sigma(F^2)]$=0.059 $wR(F^2)$=0.189
Largest differential peak andhole (e $Å^{-3}$)	0.61 and -0.56	1.20 and -0.95

Table 2a: Selected bond lengths (Å) and bond angles (°) for EDMPZC

Cl1—Zn1	2.2292 (5)	O1—Zn1	1.9649 (13)
Cl2—Zn1	2.2349 (6)	O2—Zn1	1.9472 (13)
C2—N1—C6	119.74 (14)	O1—Zn1—Cl1	114.29 (5)
C12—N11—C16	119.99 (15)	O2—Zn1—Cl2	115.09 (4)
O2—Zn1—O1	98.22 (6)	O1—Zn1—Cl2	105.10 (5)
O2—Zn1—Cl1	107.99 (5)	Cl1—Zn1—Cl2	115.06 (2)

Table 2b: Hydrogen-bond geometry (Å, °)

D—H···*A*	*D*—H	H···*A*	*D*···*A*	∠*D*—H···*A*
C8—H8*A*···O1^{i}	0.96	2.53	3.344 (3)	143
C10—H10*A*···Cl1^{ii}	0.96	2.82	3.740 (2)	162
C10—H10*C*···Cl1^{iii}	0.96	2.82	3.745 (2)	162
C13—H13···Cl2iv	0.93	2.82	3.709 (2)	161

Table 3a: Selected bond lengths (Å) and bond angles (°) for EDMPZB

O1—Zn1	1.957 (3)	Zn1—Br	2 2.3501 (8)
O2—Zn1	1.976 (3)	Zn1—Br1	2.3635 (8)
O1—Zn1—O2	101.12 (13)	O2—Zn1—Br1	108.20 (10)
O1—Zn1—Br2	111.24 (11)	Br2—Zn1—Br1	117.46 (3)
O2—Zn1—Br2	108.65 (10)	C6—N1—C2	119.7 (4)
O1—Zn1—Br1	108.88 (10)	C16—N11—C12	120.0 (3)

Table 3b: Hydrogen-bond geometry (Å, º)

D—H···*A*	*D*—H	H···*A*	*D*···*A*	∠*D*—H···*A*
C5—H5···O2	0.93	2.57	3.093 (5)	116

Table 4: Comparison of vibrational frequencies of EDMPZC, EDMPZB and EDMP

Wavenumber (cm^{-1}) $EDMP.3H_2O$ [12]	**EDMPZC**	**EDPMZB**	**Assignments**
3390-3185	3429	3443	υ (O−H) H-bonded
3000	2976	2992	υ (C−H)
1631	1624	1622	υ (C═O)
1549	1558	1557	υ (C−H), overtone
1525	1508	1501	υ (C═C)
1455	1479	1438	δ (C−H)
1375, 1338	1373, 1336	1378, 1337	δ (C−H of CH_3)
1198, 1183	1195, 1181	1197, 1171	υ (C−N) or ρ(C−H)
1034	1032	1029	υ (C−N)
881, 848	869, 842	876, 852	π (C−H)
697	729	731	π (C−H)
494	502	510	π (C═O)
-	452	460	υ (Zn−O)

Table 5: Comparison of chemical shifts δ (ppm) observed in EDMPZC, EDMPZB with EDMP

$EDMP.3H_2O$ [12]	EDMPZC	EDMPZB	Origin
^{1}H NMR			
1.192	1.187	1.112	
1.210	1.205 (triplet)	1.135	CH_3 (ethyl)
1.228	1.223	1.156	
2.362	2.357 (singlet)	2.305	CH_3 (methyl)
3.975	3.970	3.911	
3.993	3.988	3.933	
4.011	4.006 (quartet)	3.956	CH_2 (ethyl)
4.029	4.024	4.002	
4.693	4.693	4.683	H_2O
6.285	6.281 (singlet)	6.226	C−H
^{13}C NMR			
177.952	178.520	180.583	C−O
151.977	152.169	154.730	C−CH_3
116.823	116.920	119.466	C−H
43.735	43.845	46.395	CH_3 (methyl)
19.346	19.434	21.988	ethyl
13.414	13.440	15.980	ethyl

Table 6: Comparison of lower cutoff wavelength, optical transmittance window and laser damage threshold of few synthesized compounds

Compound	Lower cutoff wavelength (nm)	Optical transmittance window (nm)	Laser damage threshold (GW/cm^2)
$EDMP.3H_2O$ [12]	280	280-1100	7.6
$EDMPCl.2H_2O$ [22]	275	275-1100	3.40
$EDMPBr.2H_2O$ [22]	275	275-1100	6.36
EDMPZC*	262	262-800	29.25
EDMPZB*	263	263-800	71.16

**present work*

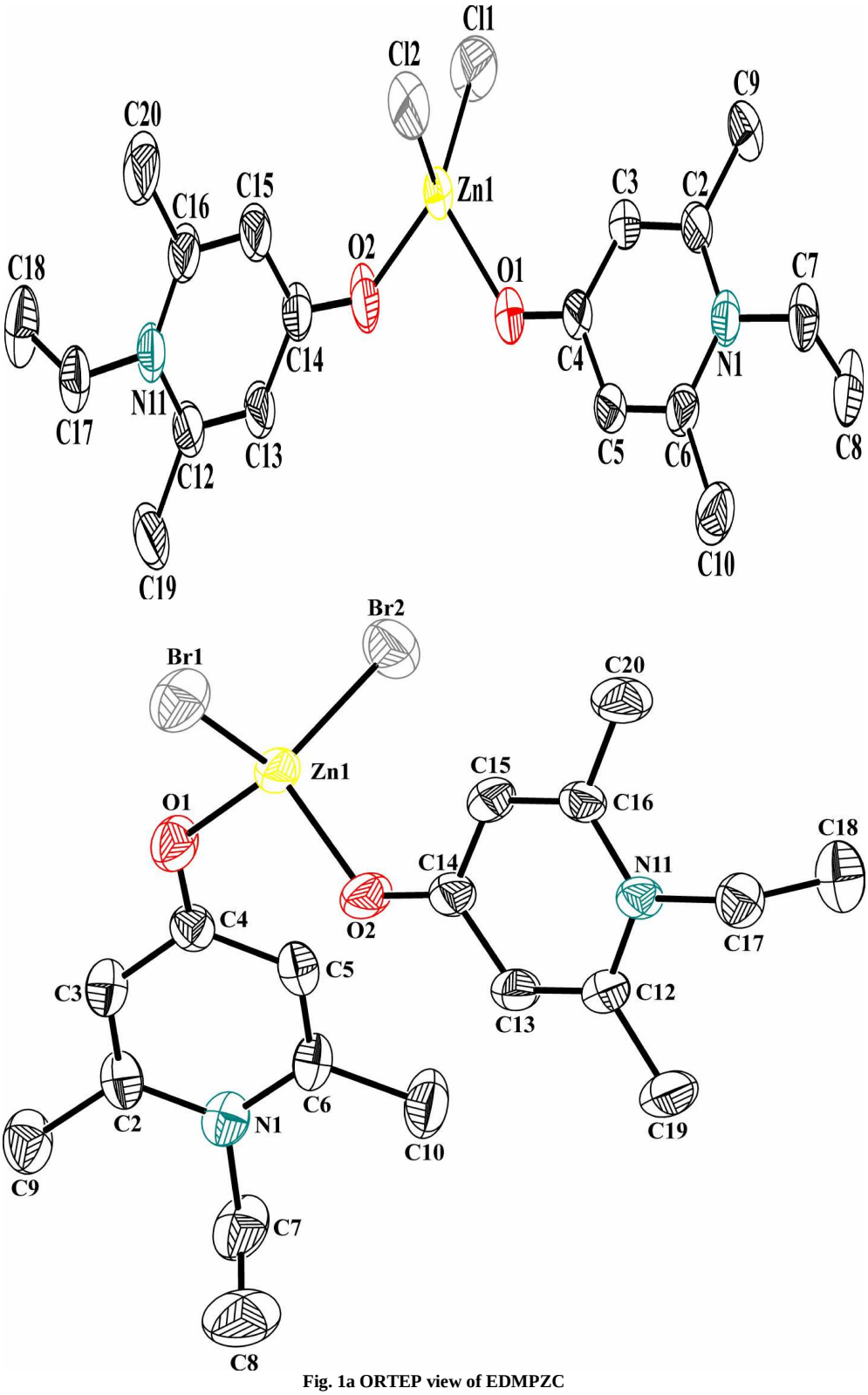

Fig. 1a ORTEP view of EDMPZC
Fig. 1b ORTEP view of EDMPZB

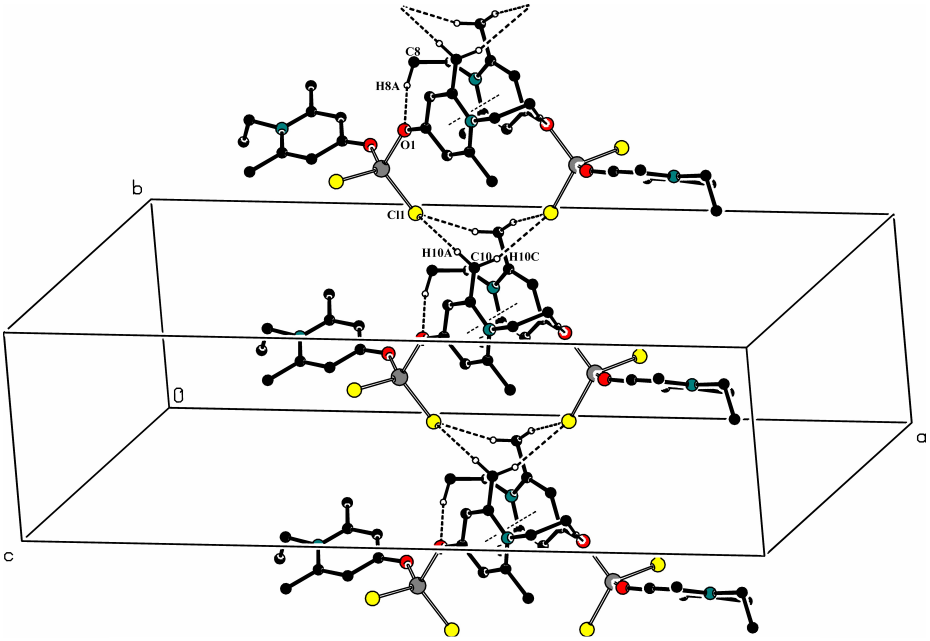

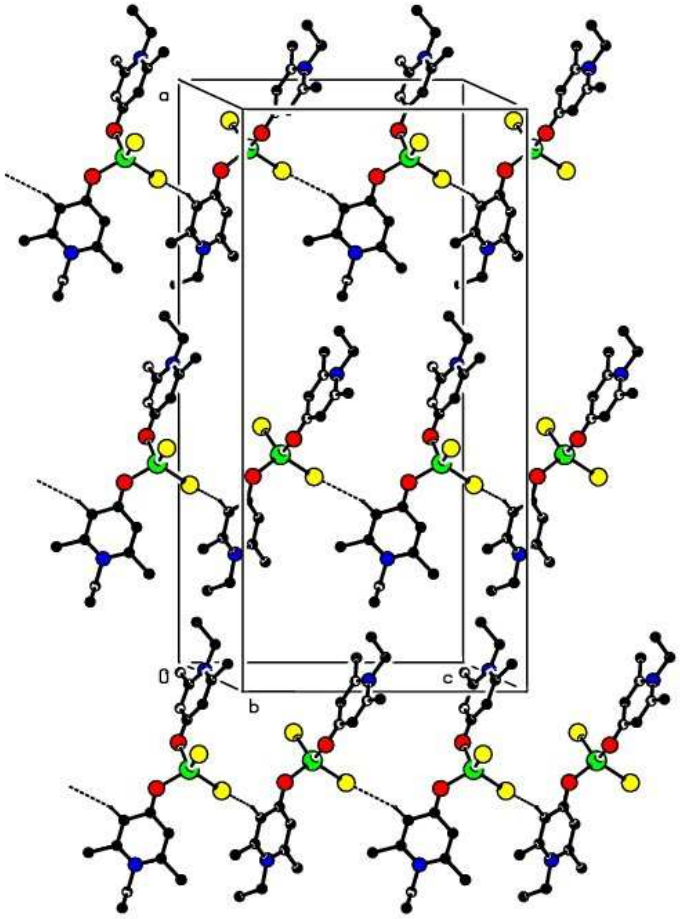

Fig. 2a Crystal packing of the molecules EDMPZC viewed down the *c*-axis.
Fig. 2b The crystal structure shows the zig–zag chain directing along *c*-axis. The dashed lines indicate the C-H···Cl hydrogen bonds of EDMPZC molecules.

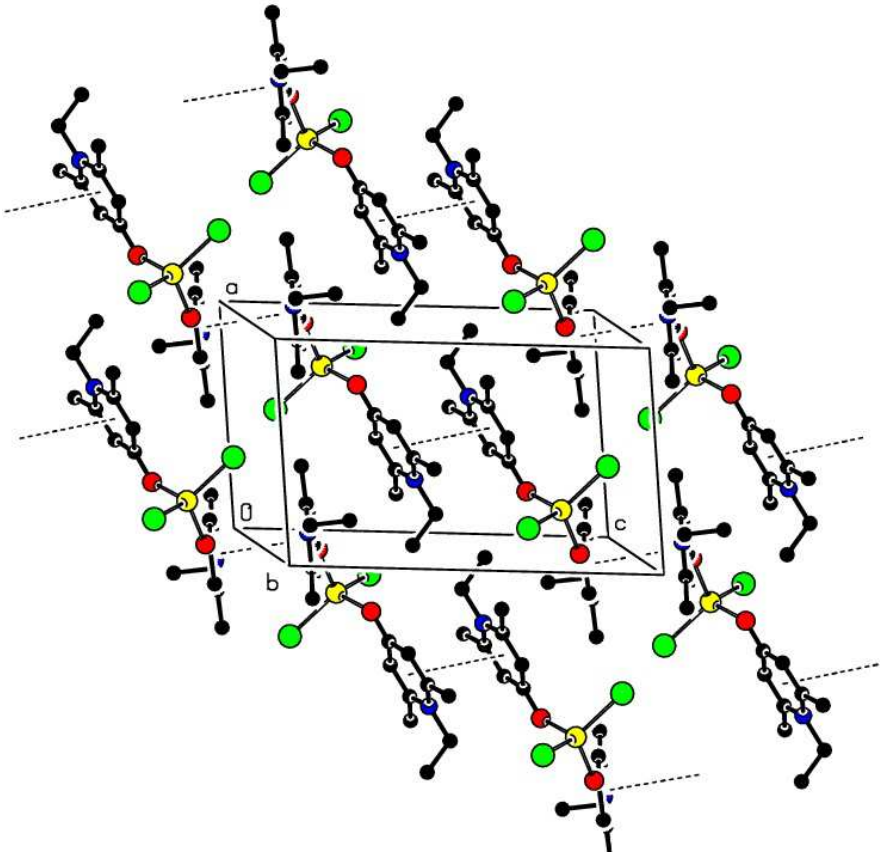

Fig. 3 The π–π interactions running diagonally along the *ac* plane of EDMPZB molecules

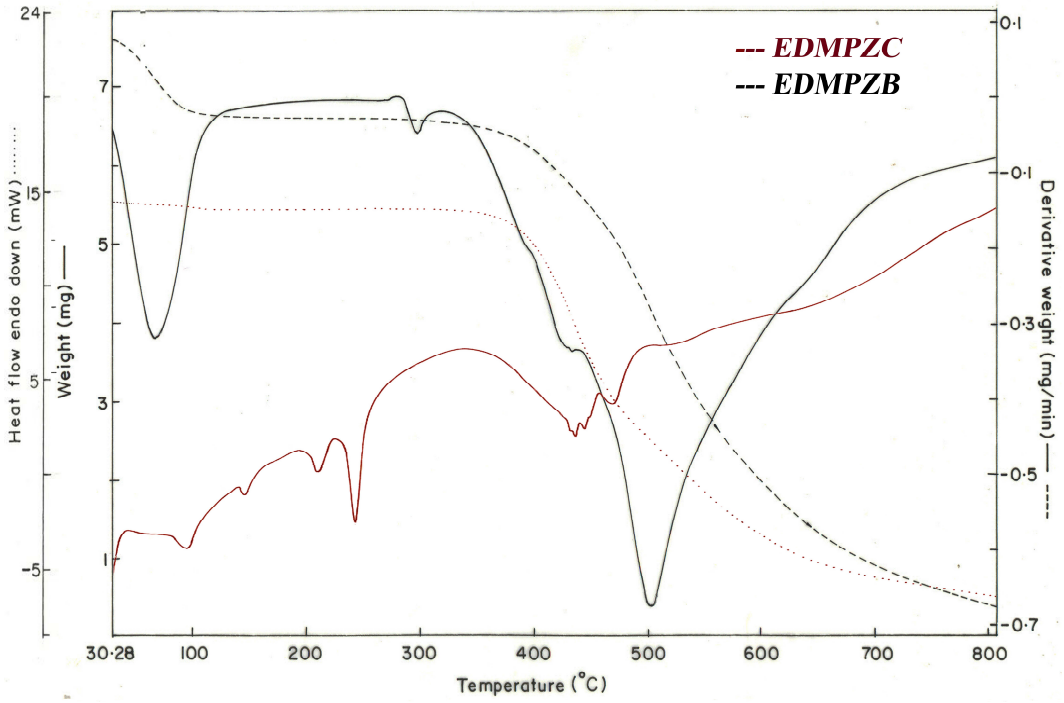

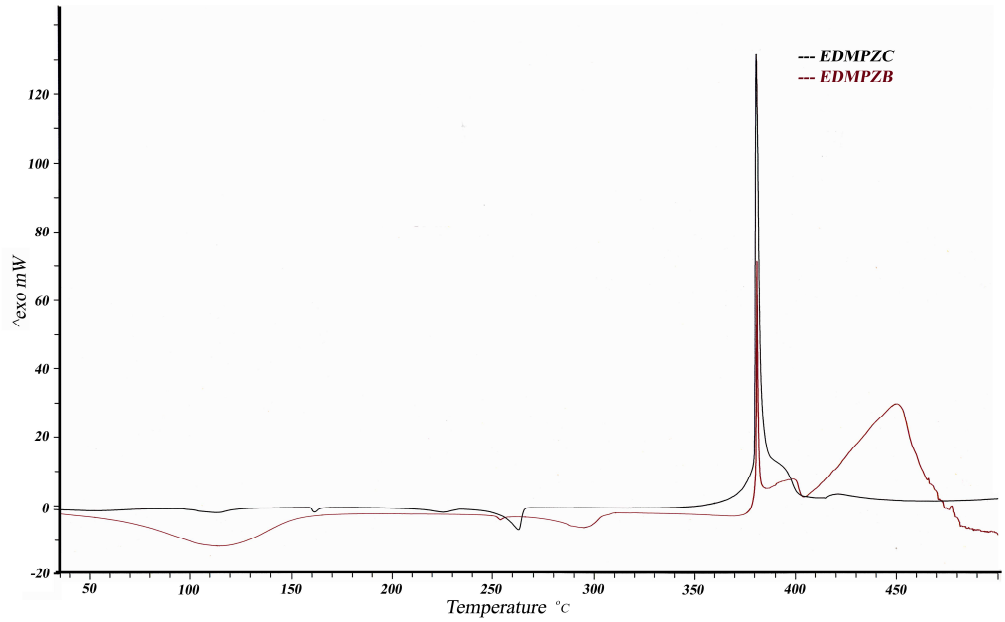

Fig. 4a Overlay TG/DTA curves of EDMPZC and EDMPZB
Fig. 4b Overlay DSC curve of EDMPZC and EDMPZB

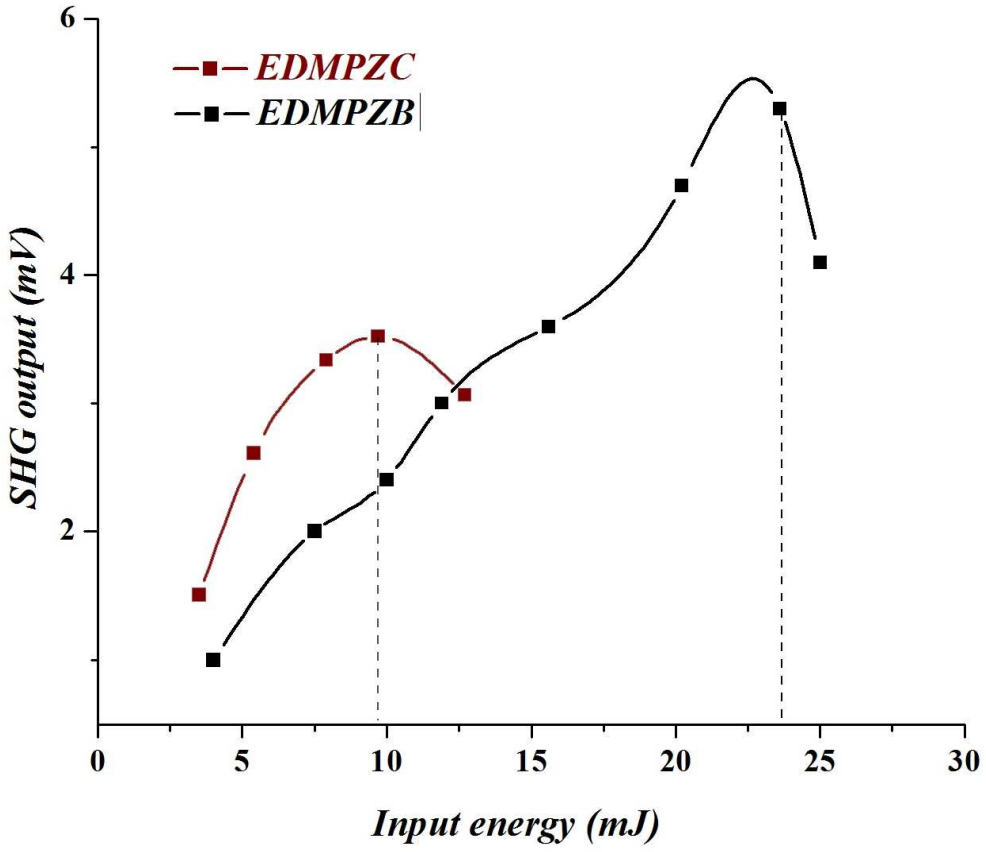

Fig. 5 Variation of SHG output against input energy for EDMPZC and EDMPZB

CONCLUSION

A novel metal – organic co-ordination compounds dichloridobis(1-ethyl-2, 6-dimethylpyridinium-4-olate-κO) zinc (II) (EDMPZC) and dibromidobis(1-ethyl-2, 6-dimethylpyridinium-4-olate-κO) zinc (II) (EDMPZB) were designed and synthesized and single crystals were grown by solvent evaporation technique. EDMPZC and EDMPZB belong to monoclinic and triclinic with the space group of C2/c and Pī respectively. The molecular structure was confirmed by FTIR and FTNMR spectral analyses. Addition of metal halides into EDMP improves the optical and thermal stability of the complexes. Transmittance window and the lower cutoff wavelength (262 nm for EDMPZC and 263 nm for EDMPZB) were identified from the linear optical studies. It is evidence that the large transmission in the UV and visible region makes the candidates suitable for optoelectronic applications and the generation of higher harmonics using Nd: YAG laser through NLO phenomena.

REFERENCES

[1] H. O. Marcy, M. J. Roskar, S. P. Velsco, C. A. Ebbers, J. H. Liao, M. G. Kanatzids, *Opt. Lett*. **1995**, 20, 252.
[2] M. H. Jiang, Q. Fang, *Adv. Mater*. **1999**, 11, 1147.
[3] P. N. Prasad, D. J. Williams, Introduction to Nonlinear Optical Effects in Organic Molecules, John Wiley & Sons, Inc., New York, **1991**.
[4] G. Kickelbick, Hybrid Materials: Synthesis, Characterization and Applications, Wiley- VCH, Weinbeim, 2007.
[5] J. T. Hupp, K. R. Poeppelmeier, *Science*, **2005**, 309, 2008.
[6] E. Y. Lee, S. Y. Jang, M. P. Suh, *J. Am. Chem. Soc*. **2005**, 127, 6374.
[7] H. Y. Lee, J. Park, M. S. Lah, J. I. Hong, *Cryst. Growth Des*. **2008**, 8, 587.
[8] Y. Yamauchi, M. Youshizawa, M. Fuzita, *J. Am. Chem. Soc*. **2008**, 130, 5832.
[9] D. R. Xiao, E. B. Wang, H.Y. An, Y.G. Li, Z.M.Su, C.Y. Sun, *Chem-Eur. J*. **2006**, 12, 6528.
[10] X. L. Wang, C. Qin, E. B. Wang, L. Xu, Z. M. Su, C. W. Hu, *Angew. Chem, Int. Ed*. **2004**, 43, 5036.
[11] Y. L. Fur, R. E. Masse, M. Z. Chekaoui, J. F. Nicoud, Z. *Kristallogr*. **1995**, 210, 856.
[12] S. Manivannan, S. K. Tiwari, S. Dhanuskodi, *Solid State Commun*. **2004**, 132, 123.
[13] J. Fan, W. Y. Sun, T.-a. Okamura, W. X. Tang, N. Veyama, *Inorg. Chem*. **2003**, 42 3168.
[14] J. Fan, I. Gan, H. Kawaguchi, W. Y. Sun, K. B, W. X. Tang, *Eur. J. Chem*. **2003**, 9 3965.
[15] W. Zhao, J. Fan, Y. Song, H. Kawaguchi, T.-a. Okamura, W. Y, Sun, N. Veyama *Dalton Trans*, **2005**, 1509.
[16] M. Thenmozhi, A. Philominal, S. Dhanuskodi, M. N. Ponnuswamy, *Acta Cryst.*, E, **2010**, 66, m1448.
[17] M. Thenmozhi, A. Philominal, S. Dhanuskodi, M. N. Ponnuswamy, *Acta Cryst.*, E, **2010**, 67, m103.
[18] A. Philominal, S. Dhanuskodi, Reji Philip, *Current Applied Physics*, **2012**, 12, 401.
[19] S. Garratt, *J. Org. Chem.*, **1963**, 28, 1886.
[20] T. V. Sundar, V. Parthasarathi, K. Sarkunam, M. Nallu, B. Walfort, H. Lang, *Acta Cryst. C*, **2004**, 60, o464.
[21] R. L. Beddoes, L. Dalton, T. A. Joule, O. S. Mills, J. D. Street, C. I. F. Watt, *J. Chem. Soc. Perkin Trans*., **1986**, 2, 787.
[22] S. Dhanuskodi, S. Manivannan, K. Kirschbaum, *Spectrochimica Acta Part* A, **2006**, 64, 504.
[23] H. Nakatani, W. R. Bosenberg, L. K. Cheng, C. L. Tany, *Appl. Phys. Lett*., **1998**, 53, 2587.